Research Square

Preprints are preliminary reports that have not undergone peer review.
They should not be considered conclusive, used to inform clinical practice,
or referenced by the media as validated information.

AoI-Optimized Lyapunov Coupling Scheduling with Channel Awareness for Precision Agriculture Heterogeneous Wireless Sensor Networks

Meiting Cai
Zhongshan Torch Polytechnic
Jinwei Zhang
Guizhou College of Electronic Science and Technology
Xin Gu
Guizhou College of Electronic Science and Technology
Zhenxing Liu
liuzhenxing87@163.com

Zhongshan Torch Polytechnic

Research Article

Keywords: Heterogeneous Wireless Sensor Networks, Age of Information, Lyapunov Scheduling, Multi-priority Traffic

Posted Date: November 19th, 2026

DOI: https://doi.org/10.21203/rs.3.rs-11450586/v1

License: This work is licensed under a Creative Commons Attribution 4.0 International License.
Read Full License

Additional Declarations: No competing interests reported.

AoI-Optimized Lyapunov Coupling Scheduling with Channel Awareness for Precision Agriculture Heterogeneous Wireless Sensor Networks

Meiting Cai[1], Jinwei Zhang[2], Xin Gu[2], Zhenxing Liu[1*]

[1]Internet of Things Application Technology, Zhongshan Torch Polytechnic, Zhongshan, 528400, China.
[2]Guizhou College of Electronic Science and Technology, Guizhou, 550000, China.

*Corresponding author(s). E-mail(s): liuzhenxing87@163.com;

Abstract

Traditional scheduling schemes fail to jointly handle static channel differences, time-varying multipath loss and multi-priority queue congestion in heterogeneous sensor networks, which raises high-priority AoI and weakens data timeliness. This paper proposes a Channel-Aware Lyapunov Coupling Stable strategy to co-optimize channel allocation and queue management. Comparative experiments on a three-layer heterogeneous scenario show that the proposed method effectively improves data timeliness and latency stability, mitigates high-priority congestion, adapts robustly to dynamic transmission loss, and maintains service fairness with optimal comprehensive performance. The proposed method provides a practical technical approach for low-latency and high-reliability data transmission in heterogeneous wireless sensor networks, and has important promotion value and application prospects for the development of precision agriculture, industrial Internet of Things, and smart city wireless transmission network industries.

Keywords: Heterogeneous Wireless Sensor Networks, Age of Information, Lyapunov Scheduling, Multi-priority Traffic

1 Introduction

Wireless sensor networks (WSNs) have been widely deployed in various fields due to their flexible deployment and low-cost advantages [1–3], and various techniques such as fault-tolerant data aggregation have been developed to improve network reliability [4]. In particular, precision agriculture has become one of the most important application scenarios of WSNs, where distributed sensors collect environmental and crop data to support intelligent decision-making [5, 6]. A vast number of distributed sensors are deployed in wide-area farmlands to continuously collect sensing data such as soil moisture, temperature, humidity, and crop growth status. The system needs to receive sensing data and distribute them to agricultural applications; services such as water-fertilizer regulation and pest and disease early warning have stringent requirements for the timeliness of the entire data reception and publication process. Information timeliness is constrained by channel communication conditions [7–9], while farmland terrain obstructions and differences in node deployment distances cause differentiation in the communication environment of sensing nodes, forming three typical types of channels: short-range line-of-sight (LOS) stable channels [10], long-range non-line-of-sight (NLOS) shadow fading channels [11], dynamic time-varying fading channels [10], and scenarios with queue backlog [8]. Changes in the communication environment directly affect the transmission success rate and communication quality of each node, easily causing problems such as mixed old and new data and invalid decision-making basis [12]. To quantify data freshness, the industry has introduced Age of Information (AoI) as a core metric [13–15].

To address the above challenges in heterogeneous wireless sensor networks for precision agriculture, this paper proposes the CA-LCS (Channel-Aware Lyapunov Coupling Stability) scheduling algorithm based on Lyapunov optimization theory, integrating three core innovation mechanisms: introducing a channel awareness module to obtain node communication quality in real time; constructing a dynamic node priority strategy to balance scheduling opportunities between strong and weak channel nodes; adding multi-queue coupled cooperative scheduling constraints to achieve system-level joint optimization across the network. The rest of this paper is organized as follows. Section 2 reviews related work on AoI scheduling. Section 3 describes the heterogeneous wireless sensor network system model and parameter settings. Section 4 presents the proposed CA-LCS algorithm in detail. Section 5 analyzes the performance characteristics of the proposed method. Finally, Section 6 concludes the paper.

2 Related Work

Scholars worldwide have conducted extensive research on AoI-optimal scheduling, forming three mainstream technical routes. As a new metric for quantifying information freshness, AoI has been systematically studied in various network scenarios [16, 17]. The first is static rule-based scheduling, with round-robin scheduling as a typical representative [7]. This method is simple to implement and has strong stability, but its scheduling strategy is fixed and cannot perceive real-time channel status and data freshness, making it difficult to balance overall network AoI performance in networks with significant differences in channel quality. The second is dynamic scheduling

based on greedy rules, mainly including instantaneous AoI greedy scheduling [13] and channel-priority greedy scheduling [18]. The instantaneous AoI greedy strategy prioritizes scheduling nodes with the oldest information, only focusing on data timeliness while ignoring channel transmission conditions; continuously scheduling nodes with poor channels will cause frequent transmission failures and aggravate system burden. The channel-priority greedy strategy tends to serve near-end nodes with good channel conditions, causing far-end weak-channel nodes to be deprived of transmission opportunities for a long time, resulting in severe scheduling unfairness. Researchers have also investigated AoI performance under error-prone transmissions [19] and energy harvesting constraints [20], further enriching the theoretical system of AoI optimization. The third is online optimization scheduling schemes, among which scheduling algorithms based on Lyapunov drift optimization [21, 22] have received widespread attention. The Lyapunov optimization framework, as a powerful tool for stochastic network optimization [23], does not require pre-obtaining channel statistics and can realize real-time online decision-making, adapting to time-varying IoT environments. Existing research has introduced Lyapunov optimization into AoI scheduling problems, achieving long-term system performance optimization by constraining queue backlog [8], and has also explored status update systems with packet management and service deadlines [24].

Although Lyapunov optimization schemes have outstanding advantages, existing Lyapunov-based AoI scheduling mechanisms still have obvious shortcomings: most schemes lack real-time channel awareness capability and cannot fully utilize node instantaneous channel information to assist decision-making; unified scheduling weights are generally adopted, lacking dynamic priority differentiation for near and far heterogeneous nodes; meanwhile, the idea of coupled cooperative regulation among multiple queues is lacking. When applied to wide-area smart agriculture heterogeneous wireless sensor network scenarios, traditional Lyapunov scheduling cannot balance the needs of near-end and far-end nodes, easily causing a sharp rise in peak AoI of far-end nodes and a decline in network fairness.

3 Heterogeneous Wireless Sensor Network System

This paper considers a single-hop time-slotted heterogeneous wireless sensor network architecture for precision agriculture, containing $N = 30$ sensing nodes and 1 base station, with carrier frequency $f_c = 2.4$ GHz, total bandwidth $B = 9$ MHz, time slot length $\tau = 0.1$ s, total duration $T = 500$ s (5000 time slots total), and maximum concurrent transmissions per time slot $K = 3$. Such single-hop WSN architectures are widely adopted in IoT applications with standardized protocol stacks [25]. The channel model adopts the 3GPP TR 36.942 path loss model [11]. For line-of-sight (LOS) links, path loss is:

$$PL_{\mathrm{LOS}}(d) = 22.7 \log_{10}(d) + 41.0 + 20 \log_{10}(f_c/1000) \tag{1}$$

For non-line-of-sight (NLOS) links, path loss is:

$$PL_{\mathrm{NLOS}}(d) = 36.7 \log_{10}(d) + 35.3 + 26 \log_{10}(f_c/1000) + n_w \cdot L_w \tag{2}$$

where d is the transceiver distance (km) and n_w is the number of wall penetrations. Shadow fading follows a zero-mean lognormal distribution with standard deviation σ_{SF}. The time-varying characteristics of wireless channels can also be characterized by Markov models [26]. The system uses Bernoulli random packet loss to characterize wireless transmission failure events. The relationship between packet loss rate and signal-to-noise ratio is:

$$P_{\mathrm{loss},i}(t) = \frac{1}{1 + \exp(\beta \cdot (\mathrm{SNR}_i(t) - \gamma_0))} \tag{3}$$

Node transmission success rate is $P_{\mathrm{success},i}(t) = 1 - P_{\mathrm{loss},i}(t)$, consistent with the channel reliability modeling approach in [10]. Channel and network parameters are detailed in Table 2.

Table 1 Channel and Network Parameters

Symbol	Parameter Meaning	Value / Formula
N	Number of sensor nodes	30
K	Max concurrent transmissions	3
τ	Time slot length	0.1 s
T	Total duration	500 s (5000 slots)
f_c	Carrier frequency	2.4 GHz
B	Total bandwidth	9 MHz
P_{tx}	Transmit power	Scenario-dependent
σ_{SF}	Shadow fading std	8 dB
L_w	Wall penetration loss	10 dB/wall
β	Packet loss slope	2
γ_0	SNR threshold	0 dB
$Q_{\max}$	Maximum queue capacity	50 packets

To fully reproduce the transmission problems of three typical communication scenarios in wide-area farmland heterogeneous wireless sensor networks: static near-far channel differences, dynamic time-varying multipath fading, and multi-node queue backlog congestion, this paper constructs three independent scenarios on the above system platform. The core configurations of the three scenarios, including spatial deployment rules, channel transmission conditions, and node service loads, are summarized in Table 1, and the overall architecture and topology of the scenarios are shown in Figure 1. Figures 1(a)–(c) correspond to the three types of farmland sensor network transmission scenarios described above, and the visual elements such as node symbols, communication links, and embedded channel waveforms in the figures all have clear physical meanings.

Figure 1(a) shows the spatial deployment of the differentiated static channel scenario. To verify the algorithm's adaptability to static channel differences, this scenario sets the node transmit power fixed at 5 dBm (see Table 1 for details), and the baseline signal-to-noise ratio (SNR) of all sensing nodes remains constant, with channel state unchanged over time. In the figure, BS represents the base station, deployed at the center of the scenario, circular symbols represent sensing nodes, totaling 30, divided into two groups according to distance from the base station: 10 near-end nodes are

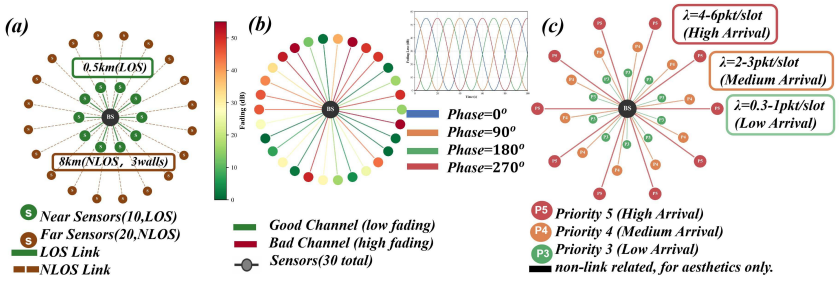


Fig. 1 Three signal transmission scenarios. (a) Differentiated channel quality: sensors at different distances with wall obstructions form LOS and NLOS links. (b) Propagation loss scenario: signals undergo multipath reflection, and a sinusoidal fading model [10] (top-right inset) with diverse initial phases is adopted to reproduce the time-varying propagation loss. (c) Queue congestion scenario: high-priority sensors with the maximum packet arrival rate generate packets beyond system transmission capacity and suffer queue congestion, whereas medium-priority sensors have moderate load and low-priority sensors carry light traffic. Connecting lines are layout decorations without distance-related physical meaning.

deployed adjacent to the base station (green circles in Figure 1(a)), with a transceiver distance of 0.5 km, using line-of-sight (LOS) links with no wall penetrations, 20 far-end nodes are deployed on the outer ring of the scenario (brown circles in Figure 1(a)), with a transceiver distance of 8 km, with 3 wall penetrations, using non-line-of-sight (NLOS) links. The lines between nodes and the base station in the figure only indicate spatial layout and do not represent distance scale.

Figure 1(b) shows the spatial deployment and channel characteristics of the time-varying multipath fading scenario. To simulate the low-power operation mode under resource constraints, this scenario sets the transmit power to -10 dBm, with a fading period of 50 time slots and a fading depth of 55 dB, and the instantaneous packet loss probability of nodes changes continuously over time slots (see Table 1 for details). Thirty sensing nodes are uniformly deployed on a circle with the base station as the center and radius $d = 2$ km, and all links have no wall obstructions, using LOS line-of-sight links. Multiple colors are used to mark sensing nodes in the figure, with different colors corresponding to initial channel states randomly assigned to each node; to reproduce the channel differences caused by multipath scattering and signal diffraction in real environments, the initial phases of all nodes are randomized. The inset in the upper right corner of Figure 1(b) shows the sinusoidal multipath fading model, with four color curves corresponding to four initial phases, characterizing differentiated channel attenuation variation patterns.

Figure 1(c) shows the spatial deployment and service classification of the multi-priority queue congestion scenario. To verify the network-wide collaborative optimization capability of the scheduling algorithm under multi-queue coupled backlog conditions, this scenario sets the transmit power to 0 dBm, and all node links have no wall obstructions, using LOS line-of-sight communication links (see Table 1 for details). A total of 30 sensing nodes are configured, evenly divided into three groups: red circles represent 10 high-arrival-rate nodes (priority P5), with packet arrival rates of 4–6 pkt/slot; orange circles represent 10 medium-arrival-rate nodes (priority P4), with packet arrival rates of 2–3 pkt/slot; green circles represent 10 low-arrival-rate

nodes (priority P3), with packet arrival rates of 0.3–1 pkt/slot. Differentiated packet arrival rates of different groups of nodes cause varying degrees of backlog in each node's data queue, thereby constructing a simulation environment with multiple coexisting queues and unbalanced loads. The lines between nodes and the base station in the figure are only used to show the network topology layout and do not represent actual distance scale.

The complete configuration parameters of the three scenarios are summarized in Table 1, facilitating horizontal comparison of differences in dimensions such as distance, link type, transmit power, priority distribution, arrival rate, fading model, and queue capacity.

Table 2 Configuration of Three Heterogeneous Simulation Scenarios

Configuration Item	Scenario 1: Static Channel Difference	Scenario 2: Time-Varying Multipath Fading	Scenario 3: Multi-Priority Congestion
Number of Sensors	30 (10 near + 20 far)	30 (uniform deployment)	30 (3 priority levels)
Distance d (km)	0.5 (near); 8 (far)	2 (uniform)	1–1.5 (uniform)
Link Type	LOS (near); NLOS (far)	LOS	LOS
Wall Penetrations n_w	0 (near); 3 (far)	0	0
Transmit Power P_{tx} (dBm)	5	-10	0
Priority ρ_i	3 (all identical)	3 (all identical)	{3, 4, 5}
Arrival Rate λ_i (pkt/slot)	1 (uniform)	1 (uniform)	{4–6, 2–3, 0.3–1}
Fading Model	Static (3GPP) [11]	Sinusoidal ($T_f = 50$, $A_f = 55$ dB) [10]	Static (3GPP) + Congestion Loss
Queue Capacity Q_{max}	—	—	50 packets

4 The Proposed CA-LCS Algorithm

Figure 2 shows the complete scheduling flow of CA-LCS, which characterizes the data flow logic from top to bottom. First, all sensing nodes are traversed and their scheduling scores are calculated. The core scoring model is shown in Equation (4):

$$S_i(t) = \omega_i \cdot [V \cdot \Delta_i(t) + W \cdot Q_i(t)] \cdot P_{\text{success},i}(t)^{\alpha} \tag{4}$$

The physical quantities in the equation are defined as follows: ω_i is the stability weight, used to achieve priority differentiation and prevent static weights from completely overwhelming the AoI and queue dynamic terms, avoiding permanent starvation of low-priority nodes, with a value range set to 1.0–1.4. In Scenarios 1 and 2, there is no priority assignment, and ω_i takes the value of 1; Scenario 3 needs to solve the priority queue congestion problem, with a value range of 1.0–1.4.

$\Delta_i(t)$ is the current age of information of node i, defined as $\Delta_i(t) = t - t_{\text{last},i}$, where $t_{\text{last},i}$ is the time slot number of the most recent successful update of node i. The squared term and linear term jointly suppress the continuous rise of information age, and V is the drift penalty parameter; Scenarios 1 and 2 take $V = 10$ to balance AoI minimization and channel utilization, while Scenario 3 increases V to 15 due to high-priority traffic overload to more aggressively suppress AoI accumulation.

$Q_i(t)$ is the number of backlogged packets in the local transmission queue of node i at time t, and W is the coupling function, which incorporates the queue backlog amount into the score calculation—the more severe the backlog, the higher the score, actively alleviating node buffer congestion. In Scenarios 1 and 2, the arrival rate is uniform and the queue does not backlog, so $W = 0$ is set to disable this module; Scenario 3 enables $W = 1.0$ to prevent congested nodes from continuously preempting resources in advance.

$P_{\text{success},i}(t)$ dynamically calculates the transmission success rate based on real-time SNR, differing from the fixed channel reliability assumption in traditional scheduling, achieving automatic weight reduction for weak links, where α is the channel awareness exponent; Scenarios 1 and 2 take $\alpha = 2$ to strengthen good channel preference, while Scenario 3 takes $\alpha = 1$ to avoid excessive bias toward good channels that would starve congested nodes.

After scoring is completed, all nodes are sorted in descending order of score, with higher scores representing higher transmission priority. Then the top 3 ranked nodes are selected as concurrent transmission objects for this round, forming a split with the remaining unselected nodes.

For the selected concurrent nodes, Bernoulli trials are used to simulate transmission success or failure. Each packet transmission is an independent Bernoulli trial, with transmission success probability $P_{\text{success},i}(t)$ and failure probability $1 - P_{\text{success},i}(t)$. If transmission is successful, the node queue is cleared and AoI is reset to zero; if transmission fails, the packet remains in the queue waiting for retransmission in the next round.

For sensor nodes that are not selected for scheduling in the current time slot, their Age of Information (AoI) increases by one time slot unit with each time slot iteration. Meanwhile, newly generated sensed data packets keep arriving and enqueuing into the local buffer. The queue accumulates continuously until its length reaches the maximum buffer capacity limit $Q_{\max}$, where subsequent incoming packets will be dropped due to buffer overflow. After the AoI values and queue buffer statuses of all nodes are updated, the current time slot terminates. The simulation proceeds to the next time slot, and the scheduling decision procedure restarts iteratively until the predefined total simulation duration is reached, at which point the simulation terminates.

5 Performance Evaluation

5.1 Data Timeliness Performance Analysis

To quantify the data timeliness differences of the four scheduling strategies under different channel conditions, this paper conducts average AoI simulation tests in three

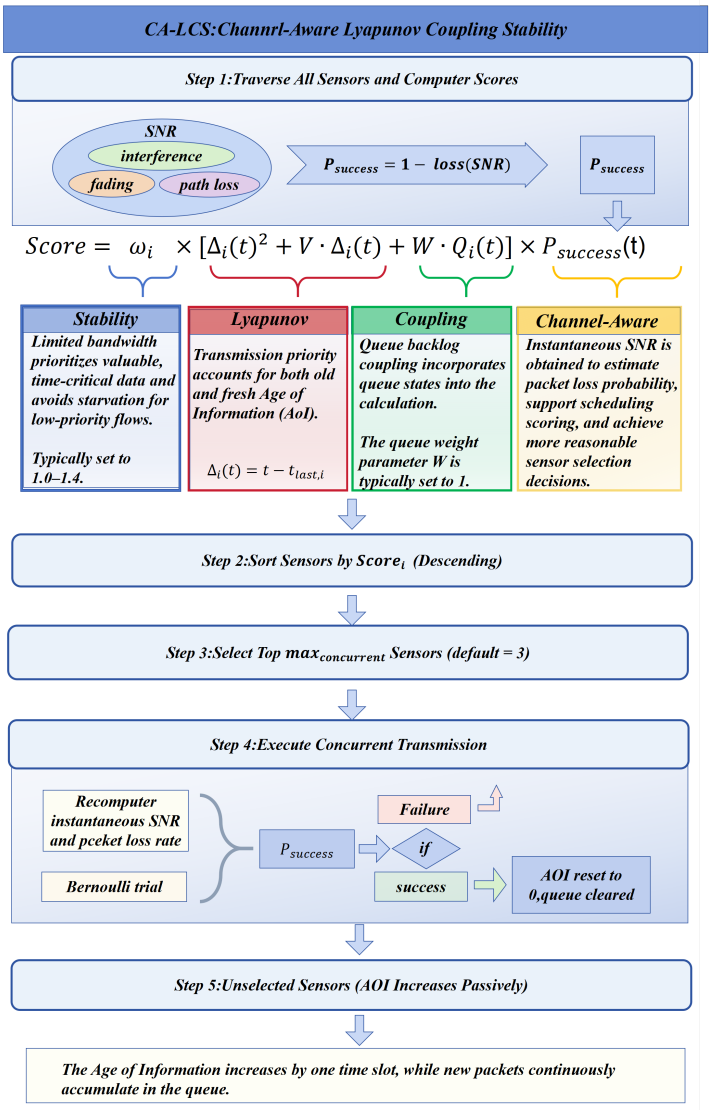


Fig. 2 The architecture of the CA-LCS scheduling algorithm. The system framework of CA-LCS comprehensively integrates four optimization components: stability weight, Lyapunov drift of Age-of-Information (AoI), queue coupling constraint, and channel-aware packet success probability.

heterogeneous scenarios, with results shown in Figure 3. The brown solid line represents round-robin scheduling, the black solid line is Max-AoI, the blue solid line corresponds to Priority-AoI, and the red solid line is the proposed CA-LCS algorithm; the horizontal axis is the simulation runtime, and the vertical axis records the real-time average AoI value. Figures 3(a)–(c) are the time-series change curves under the

three scenarios of static channel difference, time-varying multipath loss, and multi-priority queue congestion, respectively, and Figure 3(d) summarizes the average AoI statistical means of the three scenarios for horizontal quantitative comparison.

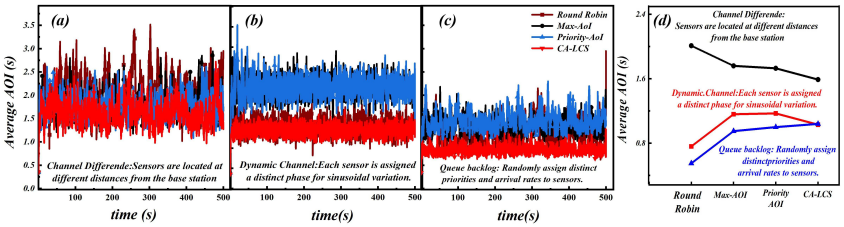


Fig. 3 Data timeliness under four scheduling algorithms. The brown line represents Round Robin, the black line denotes Max-AoI, the blue line corresponds to Priority-AoI, and the red line stands for CA-LCS. (a), (b), and (c) show the average AoI of the differentiated channel quality scenario, the propagation loss scenario, and the queue congestion scenario, respectively. (d) The relationship between average AoI and four scheduling algorithms.

In the static channel difference scenario shown in Figure 3(a), the red curve corresponding to CA-LCS remains at the lowest position among the four curves throughout the process, continuously maintaining a lower age of information. The brown line corresponding to round-robin scheduling consistently stays at a high level, because far-end NLOS nodes occupy time slots for a long time but frequently fail to transmit, leading to an increase in system average AoI. The curves of Max-AoI and Priority-AoI lie between the two, showing some improvement but lacking real-time channel awareness, unable to effectively avoid high-loss far-end links.

In the time-varying multipath loss scenario shown in Figure 3(b), the curves of the three traditional scheduling strategies show obvious fluctuations along with the sinusoidal channel fading, among which Max-AoI and Priority-AoI have the largest fluctuation amplitude, reflecting their lack of adaptability to dynamic channels. The brown line corresponding to round-robin scheduling has relatively gentle fluctuations and is overall lower, because all sensors have identical deployment conditions (distance, priority, arrival rate all consistent), and the uniform allocation strategy of round-robin naturally adapts to this symmetric scenario. The CA-LCS red curve has smaller fluctuation amplitude and is more stable when facing dynamic channels, and its overall level is second only to round-robin.

In the multi-priority queue congestion scenario shown in Figure 3(c), continuous accumulation of high-priority packets raises the average AoI of other algorithms, and the Max-AoI and Priority-AoI curves show a significant overall rise. CA-LCS actively relieves high-backlog nodes through the queue coupling term, maintaining the curve at a lower level. It should be noted that the global average AoI of CA-LCS in this scenario is slightly higher than Priority-AoI, because the algorithm actively sacrifices the timeliness of low-priority nodes to protect high-priority services.

Figure 3(d) summarizes the statistical means of average AoI over the complete simulation period of the three scenarios. In the static channel difference scenario, CA-LCS achieves the globally lowest average AoI level; under dynamic time-varying channel

conditions, CA-LCS outperforms the other comparison schemes; in the queue congestion scenario with coexisting multi-priority services, CA-LCS's optimization effect on the age of information of high-priority nodes is further highlighted. Combining the dynamic operating characteristics reflected by the time-series curves and the statistical results, it can be seen that CA-LCS jointly senses channel quality and queue backlog status for resource scheduling, which can continuously suppress the rise of system information age, and stably exerts optimization effects in static heterogeneous communication environments, time-varying multipath fading environments, and congestion scenarios with multi-service competitive access.

5.2 Data Latency Stability Performance Analysis

After completing the timeliness verification in the average AoI dimension, it is necessary to further examine the system's latency upper bound under extreme operating conditions. Peak AoI represents the worst-case transmission latency of the system, directly reflecting the stability capability of scheduling strategies to cope with burst congestion and extreme channels. Related results are shown in Figure 4. Figures 4(a)–(c) are the peak AoI time-series curves of the four algorithms under the three scenarios, with the same legend color scheme as Figure 3, and Figure 4(d) summarizes the peak AoI statistical means of the three scenarios.

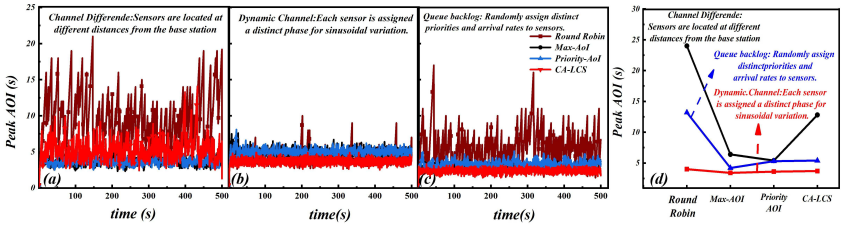


Fig. 4 Worst-case latency and latency stability under four scheduling algorithms. The brown line represents Round Robin, the black line denotes Max-AoI, the blue line corresponds to Priority-AoI, and the red line stands for CA-LCS. (a), (b), and (c) show the peak AoI of the differentiated channel quality scenario, the propagation loss scenario, and the queue congestion scenario, respectively. (d) The relationship between peak AoI and four scheduling algorithms.

In the static channel difference scenario shown in Figure 4(a), the peak AoI of the brown line corresponding to round-robin scheduling is the highest throughout, with the worst node peak AoI reaching 24.00 s, much higher than other schemes, due to continuous accumulation of far-end NLOS node queues without effective relief. Although the curves of Max-AoI and Priority-AoI are somewhat reduced, they still have obvious spikes, reflecting their lack of stable constraints on extreme channels. CA-LCS limits high-backlog nodes from continuously preempting time slots through the coupling term, while $P_{\text{success},i}$ filters out invalid weak link transmissions, maintaining peak AoI at a lower range.

In the time-varying multipath loss scenario shown in Figure 4(b), the peak AoI curves of the three traditional scheduling strategies show obvious spikes along with

deep channel fading, reflecting violent fluctuations of the worst-node latency under dynamic channels. The spike amplitude of the CA-LCS red curve is significantly smaller, with stronger latency stability when facing dynamic channels. In the multi-priority queue congestion scenario shown in Figure 4(c), Max-AoI and Priority-AoI lack queue backlog constraints, causing the peak AoI of high-priority services to rise sharply; CA-LCS relieves high-backlog nodes in advance through the queue coupling term, maintaining the peak AoI of high-priority nodes at a lower level.

The statistical results in Figure 4(d) show that the peak AoI performance of each algorithm presents obvious differentiation under different simulation scenarios. In the static channel difference scenario, the peak age of information of CA-LCS is significantly lower than the round-robin scheduling strategy; in the time-varying multipath channel environment, CA-LCS can still control peak AoI at a lower level; in the congestion scenario with coexisting multi-priority services, the algorithm's advantage in constraining peak AoI of high-priority nodes is further highlighted. Peak AoI represents the maximum information lag that may occur in the system, and the above phenomena reflect the performance differences of scheduling mechanisms. The round-robin scheme does not dynamically adjust in combination with real-time channel and queue status, easily causing continuous data update stagnation and inducing a sharp rise in AoI; CA-LCS, relying on channel awareness and queue-coupled scheduling mechanisms, can actively avoid long-term transmission vacancy problems, effectively suppress the phenomenon of extreme latency spikes, alleviate the risk of data update interruption under extreme operating conditions, and continuously ensure stable transmission of high-priority monitoring services.

5.3 Link Reliability and Slot Utilization Performance Analysis

On the basis of verifying data freshness and latency stability, this paper continues to conduct tests from two dimensions: wireless transmission reliability and time slot resource utilization. The simulation results of packet loss rate and time-domain throughput are summarized in Figure 5. Figures 5(a)–(c) correspond to the packet loss rate time-series curves under the three scenarios, with the same legend color scheme as the previous text; Figures 5(e)–(g) are the cumulative throughput change curves obtained from synchronous simulation; Figures 5(d) and 5(h) summarize the statistical results of average packet loss rate and average throughput for the three scenarios, respectively.

The packet loss rate time-series curves in Figures 5(a)–(c) show that the three traditional algorithms—round-robin, Max-AoI, and Priority-AoI—have overall higher packet loss curves. Round-robin random allocation of time slots causes a large number of time slots to be wasted on high-loss weak links, Max-AoI ignores channel quality and continuously schedules poor links, and Priority-AoI does not quantify instantaneous fading. The CA-LCS red curve maintains a lower packet loss level throughout, because the algorithm embeds real-time transmission success rate into the scoring core, prioritizing high-reliability links for transmission. The corresponding cumulative throughput curves in Figures 5(e)–(g) show that the curves of other schemes grow slowly, with a large number of time slots used for transmissions that are very likely

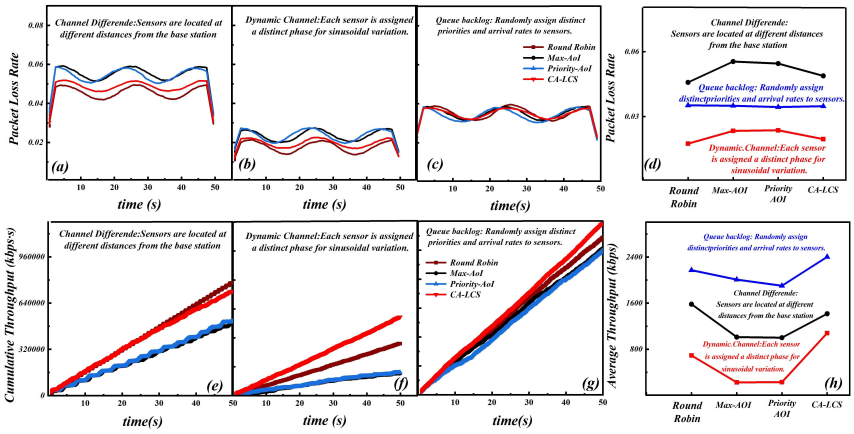


Fig. 5 Transmission reliability and slot utilization efficiency of wireless links under four scheduling algorithms. The brown line represents Round Robin, the black line denotes Max-AoI, the blue line corresponds to Priority-AoI, and the red line stands for CA-LCS. (a), (b), and (c) show the transmission reliability; (e), (f), and (g) show the slot utilization efficiency. (a) and (e), (b) and (f), (c) and (g) correspond to packet loss rate and throughput under the differentiated channel quality scenario, the propagation loss scenario, and the queue congestion scenario, respectively. (d) and (h) show the packet loss rate and the throughput vs. four scheduling algorithms.

to fail, limiting effective data growth; the CA-LCS throughput curve always leads in rising amplitude, with higher effective data transmission volume per time slot.

Figure 5(d) summarizes the average packet loss level of the algorithms under all operating conditions, and Figure 5(h) statistically obtains the average throughput of each group of strategies. Combining the two statistical subfigures, it can be seen that in static channel heterogeneous, time-varying multipath fading, and multi-priority queue congestion scenarios, CA-LCS achieves both lower average packet loss rate and higher average transmission throughput.

Analyzing from the internal mechanism of the scheduling mechanism, CA-LCS introduces a channel awareness evaluation criterion, and scheduling time slots are preferentially allocated to sensor nodes with better link transmission reliability. This strategy avoids invalid transmission attempts under weak channel conditions, reduces the probability of packet transmission failure, and at the same time avoids waste of wireless communication time slot resources, fully tapping the potential of link transmission and promoting system throughput performance improvement.

Synthesizing all simulation results from Figures 3 to 5, the following pattern can be summarized: the CA-LCS scheduling framework has obvious advantages over traditional scheduling strategies in multiple dimensions including controlling information age, constraining extreme peak latency, reducing packet loss, and improving slot throughput efficiency. It has good adaptability to three typical heterogeneous sensor network conditions: static channel differences, dynamic wireless fading, and multi-service queue congestion.

6 Conclusion

Traditional heterogeneous wireless sensor network scheduling strategies only optimize priority queuing or AoI metrics individually, unable to jointly handle the coupling problems of static channel differences, time-varying multipath loss, and multi-priority queue congestion, leading to higher age of information for high-priority services and insufficient timeliness of monitoring data. This paper proposes a Channel-Aware Lyapunov Coupling Stable scheduling strategy (CA-LCS), which constructs a scoring system from stability weight, AoI Lyapunov drift, queue backlog coupling constraint, and real-time channel transmission probability, realizing joint management of channel resource allocation and multi-priority queues.

Comparative results under three heterogeneous scenarios show that compared with three classic scheduling strategies—round-robin, Max-AoI, and Priority-AoI—CA-LCS demonstrates stable performance advantages under various operating conditions. In static channel heterogeneous environments, time-varying wireless fading environments, and multi-priority service congestion environments, the algorithm can continuously reduce system information age and effectively relieve the data queuing pressure of high-priority services, providing a feasible scheme for multi-sensor transmission scheduling optimization in smart agriculture.

Acknowledgements. The authors would like to thank the editors and anonymous reviewers for their valuable comments and suggestions that helped improve the quality of this paper.

Declarations

- **Funding**
  This work was supported by the Doctoral Workstation Program of Zhongshan Torch Polytechnic, China (Grant No. 2023BS03); the Special Innovation Program of Universities in Guangdong Province, China (Grant No. 2023KTSCX362); the Special Innovation Program of Universities in Guangdong Province, China (Grant No. 2025KTSCX382); the Special Innovation Program of Universities in Guangdong Province, China (Grant No. 2024KTSCX244); and the 2026 Guangdong Provincial Special Fund for College Students' Science and Technology Innovation Strategy (Cultivation Program for College Students' Science and Technology Innovation) (Grant No. pdjh2026bg402).
- **Conflict of interest**
  The authors declare that they have no conflict of interest.
- **Ethics approval**
  Not applicable.
- **Consent to participate**
  Not applicable.
- **Consent for publication**
  Not applicable.
- **Data availability**

The data used to support the findings of this study are available from the corresponding author upon request.

- **Code availability**
  The code used in this study is available from the corresponding author upon request.
- **Author contribution**
  All authors read and approved the final manuscript.

References

[1] Akyildiz, I.F., Su, W., Sankarasubramaniam, Y., *et al.*: Wireless sensor networks: a survey. Computer Networks **38**(4), 393–422 (2002)

[2] Yick, J., Mukherjee, B., Ghosal, D.: Wireless sensor network survey. Computer Networks **52**(12), 2292–2330 (2008)

[3] Chong, C.Y., Kumar, S.P.: Sensor networks: evolution, opportunities, and challenges. Proceedings of the IEEE **91**(8), 1247–1256 (2003)

[4] Demirbas, M., Arora, A., Mittal, V., Kulathumani, V.: A fault-local self-stabilizing clustering service for wireless ad hoc networks. IEEE Transactions on Parallel and Distributed Systems **17**(9), 912–922 (2006)

[5] Ruiz-Garcia, L., Lunadei, L., Barreiro, P., *et al.*: A review of wireless sensor technologies and applications in agriculture and food industry: state of the art and current trends. Sensors **9**(6), 4728–4750 (2009)

[6] Wang, N., Zhang, N., Wang, M.: Wireless sensors in agriculture and food industry—recent development and future perspective. Computers and Electronics in Agriculture **50**(1), 1–14 (2006)

[7] Kaul, S., Yates, R., Gruteser, M.: Real-time status: How often should one update? In: 2012 Proceedings IEEE INFOCOM, pp. 2731–2735 (2012)

[8] Costa, M., Codreanu, M., Ephremides, A.: On the age of information in status update systems with packet management. IEEE Transactions on Information Theory **62**(4), 1897–1910 (2016)

[9] Kam, C., Kompella, S., Nguyen, G.D., *et al.*: Effect of message transmission path diversity on status age. IEEE Transactions on Information Theory **62**(3), 1360–1374 (2016)

[10] Goldsmith, A.: Wireless Communications. Cambridge University Press, New York (2005)

[11] 3GPP TR 36.942 V14.0.0: Evolved Universal Terrestrial Radio Access (E-UTRA); Radio Frequency (RF) system scenarios. 3rd Generation Partnership Project (2017)

[12] Yates, R.D., Sun, Y., Brown, D.R., *et al.*: Age of information: An introduction and survey. IEEE Journal on Selected Areas in Communications **39**(5), 1183–1210 (2021)

[13] Kadota, I., Sinha, A., Uysal-Biyikoglu, E., Singh, R., Modiano, E.: Scheduling policies for minimizing age of information in broadcast wireless networks. IEEE/ACM Transactions on Networking **26**(6), 2637–2650 (2018)

[14] Buyukates, B., Soysal, A., Ulukus, S.: Age of information in multihop multicast networks. Journal of Communications and Networks **21**(3), 256–267 (2019)

[15] Hatami, M., Leinonen, M., Codreanu, M.: Aoi minimization in status update control with energy harvesting sensors. IEEE Transactions on Communications **69**(12), 8335–8351 (2021)

[16] Kosta, A., Pappas, N., Angelakis, V.: Age of information: A new concept, metric, and tool. Foundations and Trends in Networking **12**(3), 162–259 (2017)

[17] Sun, Y., Uysal-Biyikoglu, E., Yates, R.D., *et al.*: Update or wait: How to keep your data fresh. IEEE Transactions on Information Theory **63**(11), 7492–7508 (2017)

[18] Talak, R., Karaman, S., Modiano, E.: Optimizing information freshness in wireless networks under general interference constraints. IEEE/ACM Transactions on Networking **28**(1), 15–28 (2020)

[19] Kam, C., Kompella, S., Nguyen, G.D., *et al.*: Age of information under error-prone transmissions. In: 2018 IEEE International Symposium on Information Theory (ISIT), pp. 1913–1917 (2018)

[20] Yates, R.D.: Lazy is timely: Status updates by an energy harvesting source. In: 2015 IEEE International Symposium on Information Theory (ISIT), pp. 3008–3012 (2015)

[21] Kadota, I., Sinha, A., Modiano, E.: Scheduling algorithms for optimizing age of information in wireless networks with throughput constraints. IEEE/ACM Transactions on Networking **27**(4), 1359–1372 (2019)

[22] Najm, E., Yates, R., Soljanin, E.: Status updates through m/g/1/1 queues with harq. In: 2017 IEEE International Symposium on Information Theory (ISIT), pp. 131–135 (2017)

[23] Neely, M.J.: Stochastic Network Optimization with Application to Communication and Queueing Systems. Morgan & Claypool Publishers, San Rafael, CA (2010)

[24] Kaul, S., Yates, R., Gruteser, M.: Status updates through queues. In: 2012 46th

Annual Conference on Information Sciences and Systems (CISS), pp. 1–6 (2012)

[25] Palattella, M.R., Accettura, N., Vilajosana, X., *et al.*: Standardized protocol stack for the internet of (important) things. IEEE Communications Surveys & Tutorials **15**(3), 1389–1406 (2013)

[26] Zorzi, M., Rao, R.R., Milstein, L.B.: On the accuracy of a first-order markov model for data transmission on fading channels. In: IEEE ICUPC 1995, pp. 211–215 (1995)